AD-A121 424 CORROSION FATIGUE CRACK-GROWTH CHARACTERISTICS OF 1/1
SEVERAL HY-100 STEEL WE.. (U) DAVID W TAYLOR NAVAL SHIP
RESEARCH AND DEVELOPMENT CENTER ANN.. D A DAVIS ET AL.
UNCLASSIFIED OCT 82 DTNSRDC/SME-82/82 F/G 11/6 NL

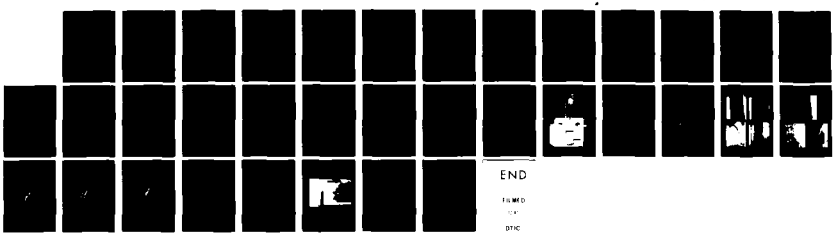

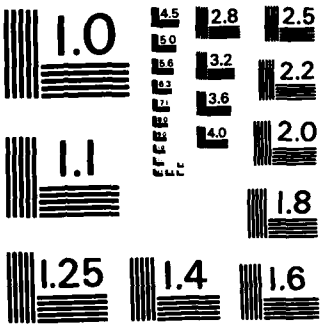

DAVID W. TAYLOR NAVAL SHIP RESEARCH AND DEVELOPMENT CENTER

Bethesda, Maryland 20084

CORROSION FATIGUE CRACK-GROWTH CHARACTERISTICS OF SEVERAL HY-100 STEEL WELDMENTS WITH CATHODIC PROTECTION

by

Dan A. Davis
E.J. Czyryca

SHIP MATERIALS ENGINEERING DEPARTMENT
RESEARCH AND DEVELOPMENT REPORT

October 1982

DTNSRDC/SME-82/82

MAJOR DTNSRDC ORGANIZATIONAL COMPONENTS

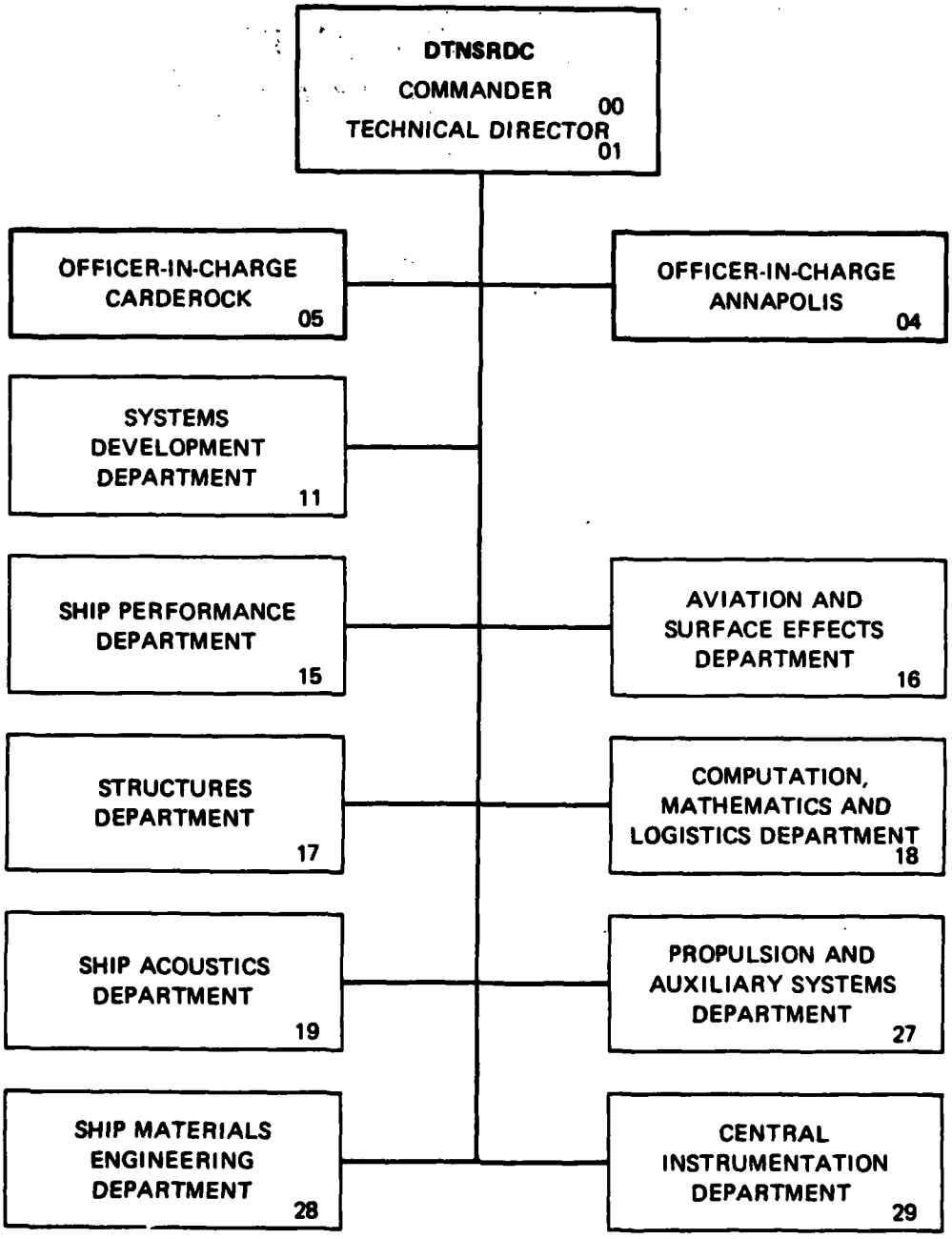

UNCLASSIFIED

SECURITY CLASSIFICATION OF THIS PAGE *(When Data Entered)*

REPORT DOCUMENTATION PAGE		READ INSTRUCTIONS BEFORE COMPLETING FORM
1. REPORT NUMBER DTNSRDC/SME-82/82	2. GOVT ACCESSION NO. AD-A122 024	3. RECIPIENT'S CATALOG NUMBER
4. TITLE *(and Subtitle)* CORROSION FATIGUE CRACK-GROWTH CHARACTERISTICS OF SEVERAL HY-100 STEEL WELDMENTS WITH CATHODIC PROTECTION		5. TYPE OF REPORT & PERIOD COVERED Research & Development 6. PERFORMING ORG. REPORT NUMBER
7. AUTHOR(s) D.A. Davis and E.J. Czyryca		8. CONTRACT OR GRANT NUMBER(s)
9. PERFORMING ORGANIZATION NAME AND ADDRESS David W. Taylor Naval Ship R&D Center Bethesda, MD 20084		10. PROGRAM ELEMENT, PROJECT, TASK AREA & WORK UNIT NUMBERS See reverse side.
11. CONTROLLING OFFICE NAME AND ADDRESS Naval Sea Systems Command (SEA 05R25) Washington, DC 20362		12. REPORT DATE October 1982 13. NUMBER OF PAGES 32
14. MONITORING AGENCY NAME & ADDRESS*(if different from Controlling Office)*		15. SECURITY CLASS. *(of this report)* UNCLASSIFIED 15a. DECLASSIFICATION/DOWNGRADING SCHEDULE

16. DISTRIBUTION STATEMENT *(of this Report)*

APPROVED FOR PUBLIC RELEASE; DISTRIBUTION UNLIMITED.

17. DISTRIBUTION STATEMENT *(of the abstract entered in Block 20, if different from Report)*

18. SUPPLEMENTARY NOTES

19. KEY WORDS *(Continue on reverse side if necessary and identify by block number)*

HY-100 Steel
Fatigue Crack Growth
Corrosion Fatigue
Cathodic Protection
Weld Metal

20. ABSTRACT *(Continue on reverse side if necessary and identify by block number)*

The corrosion fatigue crack-growth properties of several types of HY-100 steel weldments were studied, primarily in an environment of seawater with cathodic protection by zinc anode. Shielded metal-arc and gas metal-arc of both pulsed and spray-arc processes, and submerged-arc weldments were included. The fatigue crack growth tests were conducted using compact

(Continued on reverse side)

DD FORM 1 JAN 73 1473 EDITION OF 1 NOV 65 IS OBSOLETE
S/N 0102-014-6601

UNCLASSIFIED

SECURITY CLASSIFICATION OF THIS PAGE *(When Data Entered)*

Block 10

Materials Block Program - Program Element 62761N, Task Area SF-61-541-591, Work Unit 1-2803-142

HY-100 Steel Program - Program Element 63569N, Task Area S1255AS001, Task 21403 (12000), Work Unit 1-2814-157

(Block 20 continued)

specimens removed from the weldments to confine the path of the growing crack in all weld metal. Constant amplitude, sinusoidal loads were applied at a frequency of 0.17 hertz with a load ratio (minimum-to-maximum) of 0.10.

In general, fatigue crack growth in weldments was considerably slower than that in HY-100 plate under the same conditions of load and environment, where the applied potential accelerated crack-growth rate. The results showed minor differences among the weldments. It was suggested that the residual stress state along the weld center line, the inhomogeneity of the weld metal with respect to the crack path, defects, and minor porosity all act to retard crack growth, especially at lower stress intensity levels. These factors tend to mask the environmental effects. However, weldments prepared with high heat input showed greater resistance to fatigue crack propagation than weldments prepared at low heat input. The corrosion fatigue crack growth exhibited by the HY-100 weldments was similar to that of HY-80 and HY-130 weldments where weld process, environment, and loading conditions were similar.

TABLE OF CONTENTS

LIST OF FIGURES

LIST OF TABLES

LIST OF ABBREVIATIONS

ASTM	American Society for Testing and Materials
COD	Crack opening displacement
cpm	Cycles per minute
CT	Compact tension specimen
FCG	Fatigue crack growth
GMAW	Gas metal-arc welding
Hz	Hertz
kJ	Kilojoules
kN	Kilonewtons
ksi	Thousand pounds per square inch
m	Meter
mm	Millimeter
MPa	Megapascals
SAW	Submerged arc welding
SMAW	Shielded metal-arc welding

ABSTRACT

The corrosion fatigue crack-growth properties of several types of HY-100 steel weldments were studied, primarily in an environment of seawater with cathodic protection by zinc anode. Shielded metal-arc and gas metal-arc of both pulsed and spray arc processes, and submerged-arc weldments were included. The fatigue crack-growth tests were conducted using compact specimens removed from the weldments to confine the path of the growing crack in all weld metal. Constant amplitude, sinusoidal loads were applied at a frequency of 0.17 hertz with a load ratio (minimum-to-maximum) of 0.10.

In general, fatigue crack growth in weldments was considerably slower than that in HY-100 plate under the same conditions of load and environment, where the applied potential accelerated crack-growth rate. The results showed minor differences among the weldments. It was suggested that the residual stress state along the weld center line, the inhomogeneity of the weld metal with respect to the crack path, defects, and minor porosity all act to retard crack growth, especially at lower stress intensity levels. These factors tend to mask the environmental effects. However, weldments prepared with high heat input showed greater resistance to fatigue crack propagation than weldments prepared at low heat input. The corrosion fatigue crack growth exhibited by the HY-100 weldments was similar to that of HY-80 and HY-130 weldments where weld process, environment, and loading conditions were similar.

ADMINISTRATIVE INFORMATION

The work reported herein was jointly funded by the Materials Block Program and the HY-100 Steel Program. The Materials Block Program is sponsored by H.H. Vanderveldt, Naval Sea Systems Command (SEA 05R25) and funded under Program Element 62761N, Task Area SF-61-541-591, Work Unit 1-2803-142. The HY-100 Steel Program was directed by Mr. P.M. Palermo, Naval Sea Systems Command (SEA 32B) and funded under Program Element 63569N, Task Area S1255AS001, Task 21403 (12000), Work Unit 1-2814-157 The technical assistants were Mr. R. Provencher (SEA 3232) and Mr. Ivo Fioriti (SEA 3233). The effort was supervised by Mr. J.P. Gudas, David Taylor Naval Ship R&D Center (Code 2814).

This report satisfies in part Milestone RF1.5/1 of the Materials Block Program.

INTRODUCTION

HY-100 steel is a weldable, high-strength, quenched and tempered alloy steel with superior notch toughness and ductility. It is similar to HY-80, with minor adjustments to composition and heat treatment to attain higher strength. The nominal chemical composition is 0.18C-0.25Mn-0.25Si-3.25Ni-1.70Cr-0.45Mo. The objective of this investigation was to characterize the corrosion fatigue performance of HY-100 steel and weldments prepared by several welding processes. The corrosion fatigue crack-growth rates were studied in seawater, with and without applied cathodic potential.

To date, only limited fatigue data are available for HY-100 steel and weldments. The low-cycle fatigue crack initiation behavior of HY-100 plate and weldments was investigated by Gross[1*] and high-cycle fatigue and corrosion fatigue of HY-100 plate was studied by Gross and Czyryca.[2] The fatigue performance of HY-100 butt weldments was studied by Radziminski and Lawrence.[3] Only Knight[4] has investigated fatigue and corrosion fatigue crack growth of HY-100 base metal and weld metal, where crack growth was found to increase by factors up to 4.5 for base plate, manual metal-arc, and submerged-arc weld metals in a 2.6% NaCl solution. The present study complements this work by using seawater and cathodic protection as environmental variables and including a variety of welding processes.

MATERIALS INVESTIGATED

One-in. (25.4-mm)-thick[**] HY-100 plate was used in the fatigue crack-growth studies and for the preparation of single-vee butt weldments. The single-vee geometry was used to avoid incorporating root passes in the finished machined specimens and to include a large volume of weld metal in the specimen. In general, two plates, each 1 x 18 x 42 in. (25.4 x 457.2 x 1066.8 mm) were joined in the long direction, and specimen blanks were then sectioned from the completed weldment. All weldments were radiographed and were judged to be acceptable.

The welding parameters used in the fabrication of these weldments appear in Table 1. The mechanical properties of the various deposited weld metals and the base plate are listed in Table 2. These tables include similar information on an HY-80 shielded-metal-arc weldment prepared for comparison tests.

---

*A complete list of references is given on page 27.

**Defintions of abbreviations used are given on page v.

TABLE 1 - WELDING PARAMETERS FOR HY-100 AND HY-80 WELDMENTS

Type of Weldment	Configuration	Electrode Size and Type	Average Heat Input kJ/in. (kJ/mm)	Preheat/ Interpass Temperature °F(°C)	Postweld Heat Treatment
HY-100 Shielded Metal-Arc (SMAW)	Single-Vee, 35° Included Angle, 1/2-in. Root Opening	MIL-12018, 3/16-in. diam	52.5 (2.07)	225-275 (107-135)	None
HY-100 Gas Metal-Arc, Pulsed Arc (GMAW-PA)	↓	MIL-120S(Airco AX-110) 0.045 in. diam	55.7 (2.19)	275-300 (135-149)	↓
HY-100 Gas Metal-Arc, Spray Arc (GMAW-Spray)	↓	MIL-120S(Airco AX-110) 1/16 in. diam	53.3 (2.10)	275-300 (135-149)	↓
HY-100 Gas Metal-Arc, Spray Arc (GMAW-Spray)	↓	MIL-120S(Airco AX-110) 1/16-in. diam	83.9 (3.30)	275-300 (135-149)	↓
HY-100 Submerged-Arc, (SAW)	↓	MIL-120S, 1/8-in. diam	54.0 (2.13)	250-300 (121-149)	↓
HY-10Q Submerged-Arc, (SAW)	↓	MIL-120S, 1/8-in. diam	108.0 (4.25)	250-300 (121-149)	↓
HY-80 Shielded Metal-Arc (SMAW)	Single Vee, 45° Included Angle, 1/2-in. Root Opening	MIL-11018M, 1/8-in. diam	45.0 (1.77)	200-300 (93-149)	Soaked 8 hr at 200-300°C (93-149°C)

Note: 1 in. = 25.4 mm.

TABLE 2 - MECHANICAL PROPERTIES OF MATERIALS INVESTIGATED

Weldment Type Avg Heat Input kJ/in.	0.2% Offset Yield Strength ksi (MPa)	Ultimate Tensile Strength ksi (MPa)	Elongation % in 2 in. (51 mm)	Reduction in Area %	Charpy V-Notch Impact Energy at -60°F (-51°C) ft-lb (J)
HY-100 SMAW (52.5)	115.5 (796)	120.9 (834)	20	61.5	64.5 (87.5)
HY-100 GMAW-PA (55.7)	113.0 (779)	122.5 (845)	23	68.0	90.0 (122.0)
HY-100 GMAW-Spray (55.3)	114.1 (787)	123.4 (851)	21	68.0	70.0 (95.0)
HY-100 GMAW-Spray (83.9)	104.9 (723)	118.9 (820)	23	63.0	53.5 (72.5)
HY-100 SAW (54.0)	114.5 (789)	122.6 (845)	21	60.0	74.0 (100.3)
HY-100 SAW (108.0)	101.4 (699)	118.9 (820)	23	48.0	71.5 (97.0)
HY-80 SMAW (45)	-	-	-	-	-
HY-100 Plate	99.0 (682)	113.4 (78?)	25	72.0	76.0 (103.0)**

*All weld metal specimens for weldments, transverse specimens for plate.

**At -120°F (-84°C).

Note: 1 kJ/in. = 25.4 kJ/mm.

EXPERIMENTAL PROCEDURE

The fatigue crack propagation experiments were conducted with compact tension (CT) specimens similar to that described in ASTM Standard Test Method for Constant-Load-Amplitude Fatigue Crack Growth Rates Above 10^{-8} m/cycle (E647-81). In general, 1-in. (25.4-mm)-thick specimens were used with width (W) and height (H) proportioned such that H/W = 0.6, as shown in the specimen design, Figure 1. The specimen dimensions were chosen to provide for a substantial length of crack growth over which the crack-tip stress intensity does not increase rapidly under constant cyclic load. The notch and crack growth direction coincided with the rolling direction of plate and the welding direction of weldments.

The specimens were cyclicly-loaded in closed-loop, electrohydraulic fatigue machines under constant load conditions in a triangular load-wave pattern at a frequency of 10 cpm (0.17 Hz). The load ratio, $R = P_{minimum}/P_{maximum}$, was approximately 0.10. A schematic diagram of the general test arrangement is shown in Figure 2. Crack length was indirectly measured by a crack-opening displacement (COD) technique described by Yoder and coworkers.[5] The displacement gage was fixed to the specimen at the crack mouth via knife edges mounted on the specimen face.

As shown in Figure 2, a computer system was used for interactive test control, data acquisition, and on-line analysis. The software controlled specimen loading parameters and acquired 100 data pairs over one load cycle. A straight line fit to data pairs descending from maximum load was made discarding the data pairs below a cutoff level (% maximum load) where the initial portion of the load-COD plot is non-linear as determined by a display on the computer video terminal. The cutoff level was adjusted during the course of each test. The crack length was determined from the compliance (slope of the load-COD line) using the relationship developed by Saxena and coworkers[6] for CT specimens:

$$a/_W = 1.001 - 4.6695\ C + 18.46\ C^2 - 236.82\ C^3 + 1214.9\ C^4 - 2143.6\ C^5 \qquad (1)$$

where a = crack length,

W = specimen width.

$$C = 1/\left(\frac{EB_e\delta}{P}\right) + 1 \qquad (2)$$

where E = modulus of elasticity,

B_e = effective thickness = $(B \cdot B_n)^{1/2}$,

B_n = specimen thickness (net),

B = specimen thickness (gross),

δ/P = specimen compliance.

Crack-growth rates were computed by the secant method given in the appendix of ASTM E647. The crack-tip stress-intensity factor range, ΔK, was calculated from the equation given in ASTM E647 for CT specimens:

$$\Delta K = (\Delta P/B_e\sqrt{W})\left(\frac{2+\alpha}{(1-\alpha)^{3/2}}\right)\left(0.886 + 4.64\alpha - 13.32\alpha^2 + 14.72\alpha^3 - 5.6\alpha^4\right) \qquad (3)$$

where ΔP = load range, maximum load-minimum load,

$\alpha = a/W$.

As shown in Figure 1, the crack line was selected as the center line of a transverse weld in the direction of welding, thus the crack path was exclusively in weld metal. The side grooves were necessary to keep the plane of the growing crack from deviating from the crack line and to promote cracking in a single plane.

The seawater environment was contained on the specimen by means of a reservoir, as shown in Figure 3. The cyclic motion of the crack faces caused a capillary action which drew the water into the crack-tip vicinity. Although the diagram of Figure 2 suggests a vertical arrangement, the test machine was a horizontal

mounting, as shown in Figure 3. The containment reservoir was attached to one side of the specimen to allow a visual check on crack-length measurement by COD without removal of the environment. Natural seawater shipped from the LaQue Center for Corrosion Technology, International Nickel Co., Wrightsville, Beach, NC, was used. Small anodes of zinc were immersed in the reservoir and coupled to the specimen for experiments in which cathodic potentials were included. Initial tests with the anode were monitored throughout the test and provided a constant potential of -1.05 volts with respect to a saturated calomel reference cell. In all cases, the seawater was changed daily after a flush with distilled water. Due to the limited amount of material available, only one test per condition was undertaken.

The validity criteria for results expressed in terms of the linear elastic stress intensity, ΔK, for the CT specimen, given in ASTM E647-81 is expressed as:

$$W-a \geq (4/\pi)(K_{max}/\sigma_{ys})^2 \qquad (4)$$

where $W-a$ = uncracked ligament,

K_{max} = maximum stress intensity,

σ_{ys} = 0.2% offset yield strength.

The specimens of Figure 1 were cycled with a constant, maximum load of 6500 lb (28.9 kN). For HY-100 steel (σ_{ys} = 100 ksi (689.5 MPa)), ΔK is held to 92 ksi-in.^{2} (101 MPa-m$^{1/2}$) and a crack length of 2.95 in. (75 mm).

RESULTS AND DISCUSSION

The results of the fatigue crack-growth studies of HY-100 weldments are summarized and discussed in the following paragraphs. The results are primarily discussed in relation to the fatigue and corrosion fatigue crack growth characteristics of HY-100 plate which are first described. In later discussion they are compared to the corrosion fatigue crack-growth properties of HY-80 SMAW included in this study and that of HY-130 weldments previously reported.[7]

The results of fatigue crack-growth tests of HY-100 plate in air, seawater, and seawater with applied cathodic potential from zinc coupling are given in Figure 4. Both environments increased fatigue crack-growth rates significantly over the range

of stress intensity studied. The conjoint effect of seawater and electrochemical potential increased fatigue crack-growth rates by an order of magnitude compared to rates in air. Similar effects have been shown by Davis and Czyryca,[7] Crooker and coworkers,[8] and Vosikovsky[9] for HY-130 steel, as well as other high-strength steels.

The welding of HY-80 and HY-100 steels requires heat input to be limited to a maximum of 55 kJ/in. (2.2 kJ/mm). Figure 5 presents the fatigue crack-growth results for the four HY-100 weldments produced nominally within that heat input limit and tested under an environment of seawater and cathodic protection by zinc anode. In general, the shape of the fatigue crack growth curves for the weld metals (SMAW, GMAW-pulsed arc, GMAW-spray arc, and SAW) were different than for plate. Higher stress intensities were required to grow cracks in weld metal at crack growth rates below 10^{-5} in./cycle, and the rate changes from slow to faster growth rates occurred over a narrower range of stress intensity values than the plate material did. Similar behavior was observed for HY-130 steel GTA weldments tested in synthetic seawater[10] and for HY-130 SMA and GMA weldments tested in natural seawater with applied cathodic potential.[7] It should also be noted from the fatigue crack-growth data in Figure 5 that much variability exists among the curves for the various weldments.

The results shown in Figure 5 indicate that the fatigue crack-growth rates for the weldments investigated were significantly lower than those for HY-100 plate material tested under similar conditions of stress intensity and environment. Fatigue crack-growth research by Parry[11] on A514 steel weldments suggested that crack-growth rates may be reduced by compressive residual welding stresses. It is postulated that these complex residual stress patterns, along with weld porosity, defects, and metallurgical variations in the multipass weld deposits provide a tortuous, inhomogeneous path for the crack to follow, thus leading to reduced fatigue crack-growth rates in weld metal, as compared to plate. This is supported by comparing the fracture surface topographies shown macrographically in Figure 6. The fracture surface for the HY-100 plate material shows a smooth, homogeneous crack path, while those for several sample weldments exhibit jagged, inhomogeneous fracture paths with porosity. Additionally, the photomicrographs in Figure 7 show differences in microstructure, showing metallurgical variations and inclusions; and in fracture surface contour, which indicates the cracks growing in weldments did follow a more difficult, tortuous path.

Figure 8 presents fatigue crack-growth rates for HY-100 SMAW and GMAW-pulsed arc weldments (nominally 55 kJ/in. heat input) in natural seawater as well as that for the same weldments tested in seawater with applied cathodic potential. The fatigue crack-growth behavior in seawater and in seawater with cathodic potential applied were similar. It is suggested that the resistance to crack growth in these welds is caused by residual stresses and the crack path (as shown in Figure 6d) for a SMA weldment dominates the growth process, and environmental effects are of minor significance.

High heat input weldments of HY-100 steel were included in this investigation. The fatigue crack-growth rates for high-heat input GMAW-spray arc (83 kJ/in.) and SAW (108 kJ/in.) weldments tested in seawater with Zn cathodic protection are shown in Figure 9. Data for comparable tests on weldments prepared by the same processes at lower heat input are included for comparison. It is apparent that the high heat input weldments exhibit a somewhat higher resistance to fatigue crack growth in this environment. This behavior might be expected since the high heat input may lead to higher residual stress levels which, as previously discussed, tend to retard the growth of the crack. Figure 10 compares the fatigue crack-growth characteristics of these high heat input welds in seawater and coupled to zinc anode. As observed in studies of welds prepared at lower heat input, these welds exhibit similar fatigue crack-growth behavior in both environments, thus indicating environmental effects to be of secondary importance.

Figures 11 and 12 show fatigue crack-growth rates for HY-100 weldments in seawater with applied cathodic potential compared to weldments of HY-80 and HY-130[7] steels prepared by similar welding processes. HY-80, HY-100, and HY-130 SMA weldments (Figure 11) exhibit similar corrosion fatigue crack-growth characteristics. The minor divergence of the fatigue crack-growth curves for these weldments may be considered within the expected range of scatter in fatigue crack-growth data for weldments. As shown in Figure 12, the fatigue crack-growth behavior of HY-100 and HY-130 GMAW are similar. In general, these data indicate that there was no significant difference in the corrosion fatigue crack-growth behavior of HY-80, HY-100, and HY-130 SMAW and GMAW weldments.

The fatigue crack-growth rates of the materials studied in this investigation are summarized in Table 3. The results of this study indicate that fatigue crack-growth rates in HY-100 weld metals are slower than in HY-100 plate at a given stress

intensity for the same environment. It was also observed that the different weld processes exhibit significant variability in fatigue crack-growth behavior in seawater with applied cathodic potential due primarily to the complex residual stress patterns and metallurgical variations involved in multipass weldments. These factors provided a tortuous path for the growing fatigue crack to follow. This resulted in the finding that all weldments of HY-100 steel in an environment of seawater with applied cathodic potential showed a significantly better resistance to fatigue crack growth than does HY-100 plate in a similar environment. These findings parallel the results of a comparison of fatigue crack-growth rates of HY-130 steel plate and weldments in marine environments,[7] for which the results are also summarized in Table 3.

TABLE 3 - COMPARISON OF FATIGUE CRACK-GROWTH DATA FOR HY-100, HY-80 AND HY-130 STEEL PLATE AND WELDMENTS

Material	Weldment Type Heat Input (kJ/in.)	Environment*	Fatigue Crack Growth Rate da/dN (μin./cycle)** at Stress Intensity Factor Range ksi-$\sqrt{in.}$ (MPa$\sqrt{m}$) Below:			
			50 (55)	60 (66)	80 (88)	100 (110)
HY-100	Plate	Air	10	15	25	30
	Plate	SW	25	30	60	100
	Plate	SW + Zn	110	190	260	350
HY-100 WELDMENTS	SMAW (52.5)	SW + Zn	-	5	10	40
	GMAW-pulsed arc (55.7)	SW + Zn	10	15	30	50
	GMAW-spray arc (55.3)	SW + Zn	30	40	60	100
	SAW (54.0)	SW + Zn	50	100	-	-
	SMAW (52.5)	SW	-	20	50	100
	GMAW-pulsed arc (55.7)	SW	10	20	30	90
	GMAW-spray arc (83.9)	SW + Zn	5	20	40	80
	SAW (108.0)	SW + Zn	-	15	40	80
	GMAW-spray arc (83.9)	SW	5	20	40	80
	SAW (108.0)	SW	-	20	40	80
HY-80 Weldment	SMAW (45.0)	SW + Zn	-	-	15	40
HY-130 (ref 7)	Plate	Air	20	35	80	140
	Plate	SW	40	50	80	140
	Plate	SW + Zn	65	70	120	350
	SMAW (40)	SW + Zn	20	30	40	60
	GMAW (40)	SW + Zn	-	15	50	100

*SW = natural seawater; SW + Zn = natural seawater with applied cathodic potential by zinc anode.
**1 μin. = 2.54×10^{-5} mm.

Parry, et al.[11] studied fatigue crack growth in weldments of A514 steel, a steel similar to HY-100 in strength level. Reduced crack-growth rates were not observed in every test, and those showing higher growth rates approached that of A514 plate. It was found that stress-relief heat treatment resulted in a considerable increase in crack-growth rates, again approaching that of the A514 base plate. This provides a qualitative demonstration that compressive residual welding stresses are the significant factor in the reduced fatigue crack growth in weldments. The compressive residual stresses of unknown magnitude result in actual values of crack-tip stress intensity factor range and maximum less than those computed from the applied loading to a CT specimen. The influence of the residual stresses also changes continuously as the crack grows and the uncracked ligament decreases. ASTM E647-81 contains guidance for specimen type and size for use when fatigue crack-growth rate testing is conducted using materials where stress relief is not performed nor practical. In general, thin CT specimens (small B/W ratio) or center-cracked tension specimens are recommended.

HY steel weldments are not stress relieved in practice. Thus, stress-relief heat treatments were not performed in this study, where the objective was to characterize fatigue crack growth in as-welded, thick-section HY-100 weld metals. A demonstration of the relevance of these data is shown in Figure 13, the failure of an HY-100 5-in. (127-mm) wide x 2-in. (50.8-mm)-thick GMAW joint in fatigue. The beam, with weld reinforcement removed by machining, was subjected to constant amplitude, constant moment bending fatigue. Although fatigue cracks initiated in the weld metal, the path of fatigue crack growth deviated until growing in the base plate away from the heat-affected zone. The results of the crack-growth study showed that HY-100 weld metals are more resistant to fatigue crack growtn than the base plate.

CONCLUSIONS

The following conclusions are warranted from this investigation of the corrosion fatigue crack-growth behavior of HY-100 steel and weldments.

- All HY-100 weldments exhibited lower fatigue crack-growth rates than HY-100 plate in an environment of seawater with applied cathodic potential by zinc anode.

- Variability in fatigue crack-growth characteristics of the HY-100 weldments prepared by different processes and heat inputs were due to variations in residual welding stresses and metallurgical variations.

- The weld factors, primarily the residual stresses, were more significant than environmental effects on fatigue crack-growth behavior; HY-100 welds tested in seawater and in seawater with applied cathodic potential exhibited similar crack-growth rates.

- The corrosion fatigue crack-growth behavior of HY-100 weldments was similar to that of HY-80 and HY-130 weldments in the same environment.

ACKNOWLEDGMENT

The various weldments used in the preparation of specimens in this task were fabricated by the Ferrous Welding Branch (Code 2821) of this Center under the direction of Mr. R.T. Brenna and Mr. G.L. Franke. Their assistance and cooperation are gratefully appreciated.

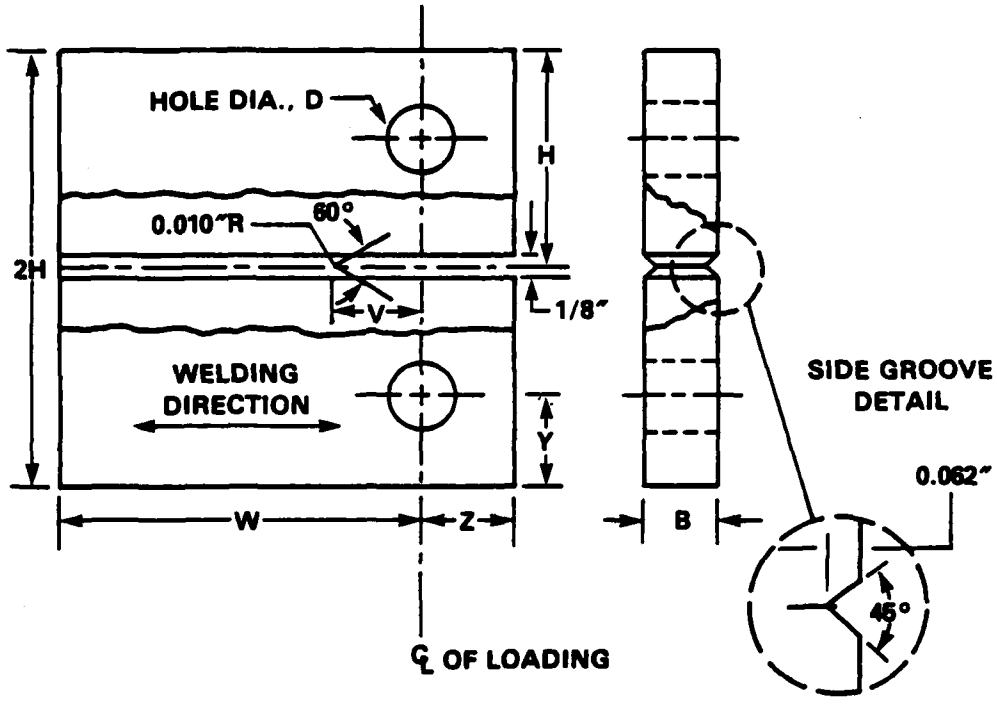

SPECIMEN TYPE	D	B	2H	V	W	H	Y	Z
4W	1(2.54)	1(2.54)	4-7/8 (12.38)	1(2.54)	4(10.16)	2-7/16 (6.19)	1(2.54)	1(2.54)

NOTE: ALL DIMENSIONS IN INCHES (cm)

Figure 1 - Compact Tension Specimen for Weld Metal Tests

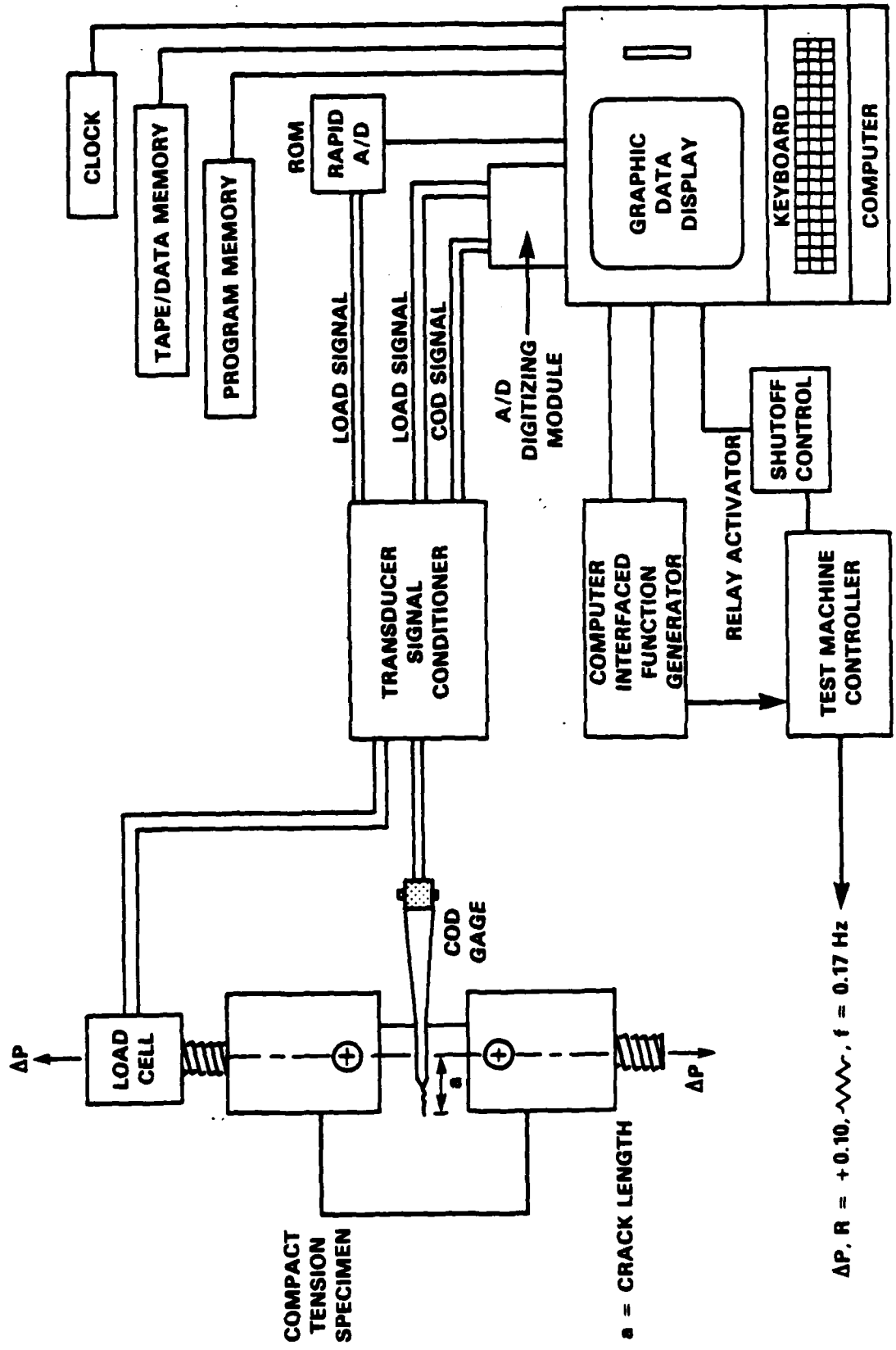

Figure 2 - Fatigue Crack-Growth Test Apparatus Including Computer Control

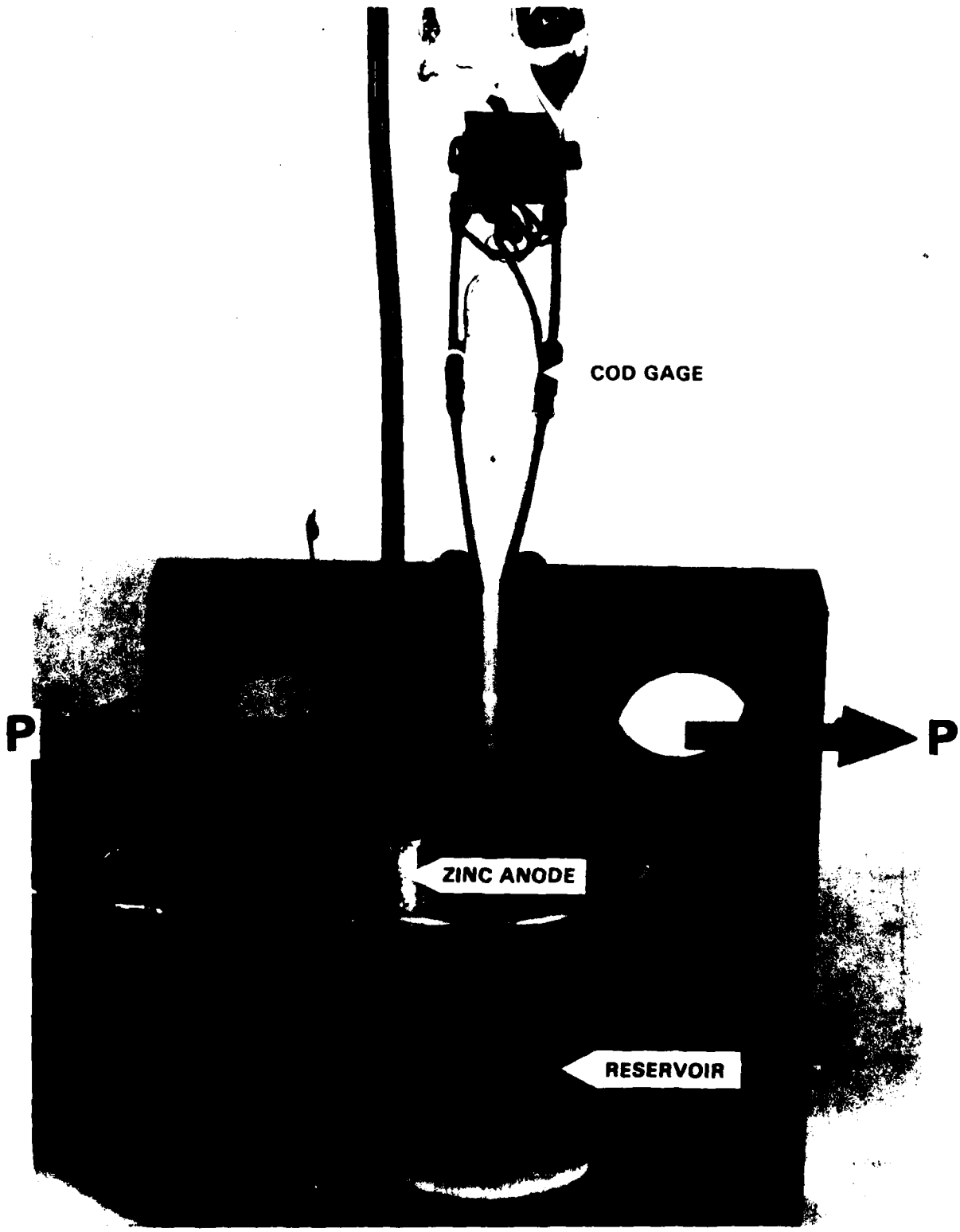

Figure 3 - Seawater Containment Reservoir and Anode Connection Setup Used on Compact Tension Specimens

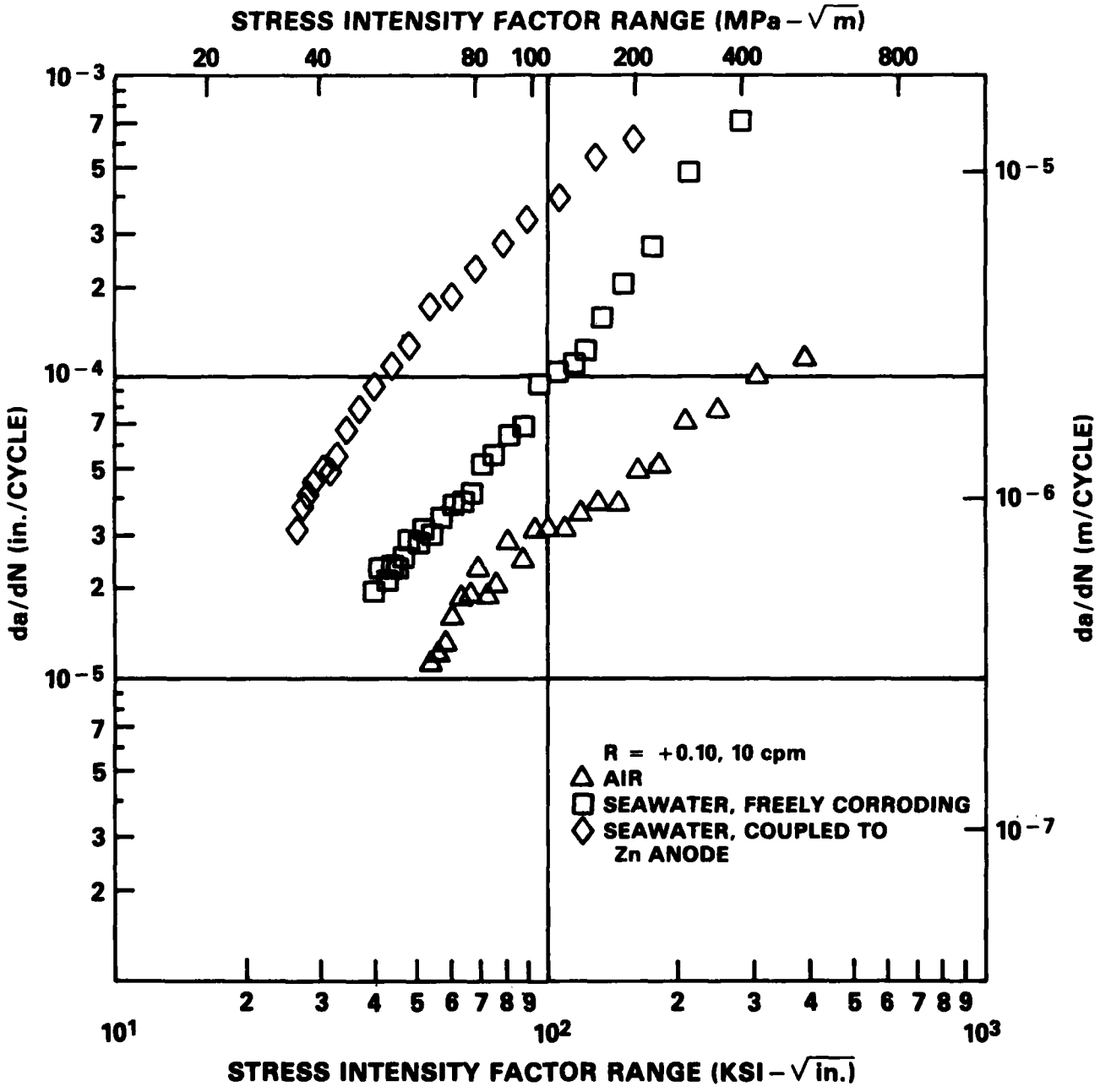

Figure 4 - Fatigue Crack-Growth Rates for HY-100 Steel Plate in Air and Natural Seawater, Uncoupled and Coupled to Zinc Anode

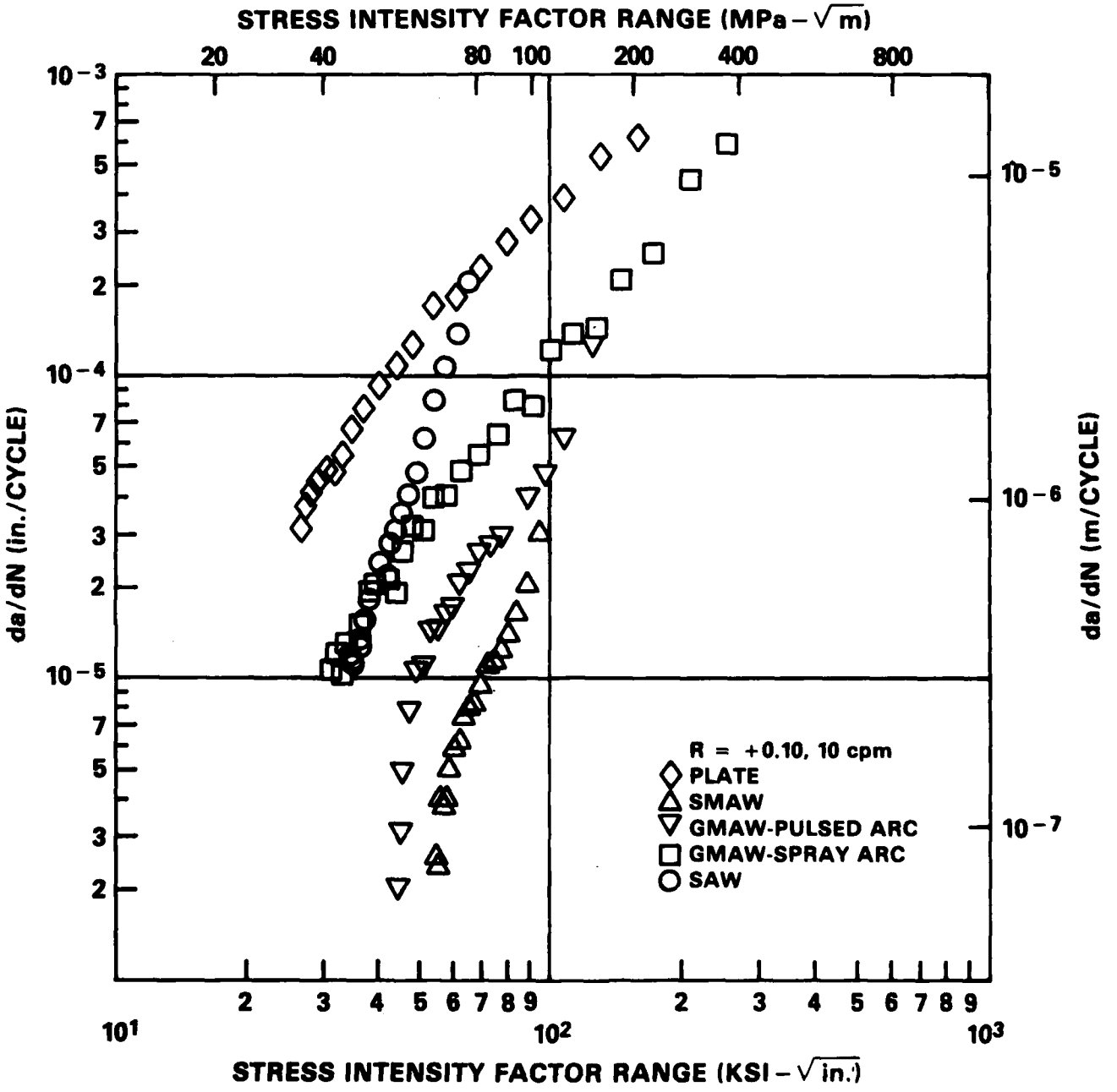

Figure 5 - Fatigue Crack-Growth Rates for HY-100 Steel Weld Metals with Heat Inputs Nominally 55 kJ/in. in Natural Seawater Coupled to Zinc Anode

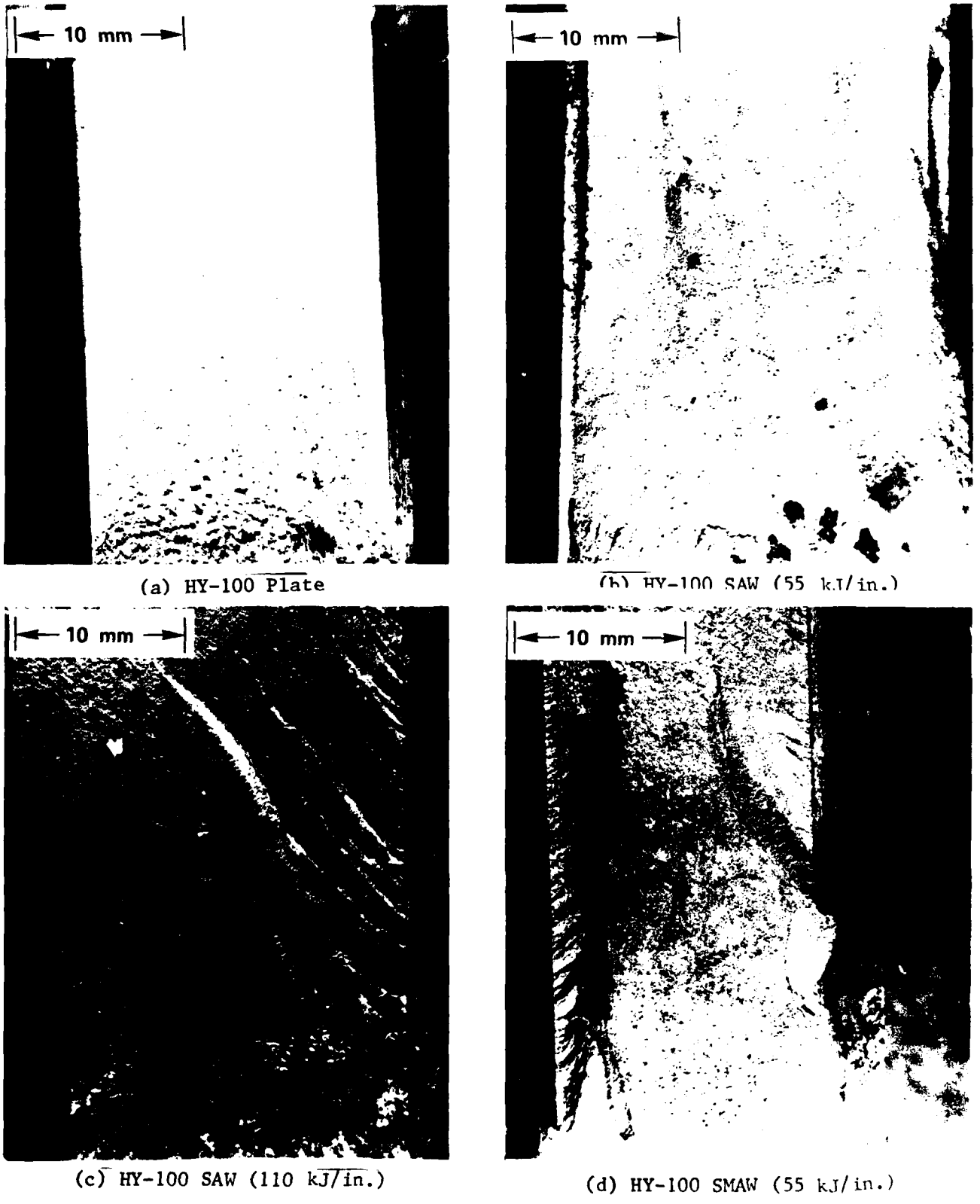

(a) HY-100 Plate

(b) HY-100 SAW (55 kJ/in.)

(c) HY-100 SAW (110 kJ/in.)

(d) HY-100 SMAW (55 kJ/in.)

Figure 6 - Fracture Surface Topography of HY-100 Steel Plate and Weld Metal Tested in Natural Seawater Coupled to Zinc Anode

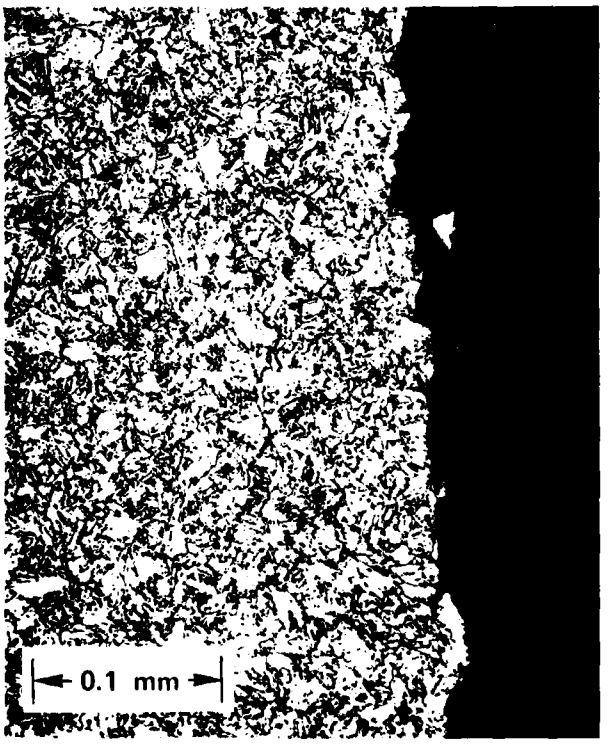

(a) HY-100 Plate

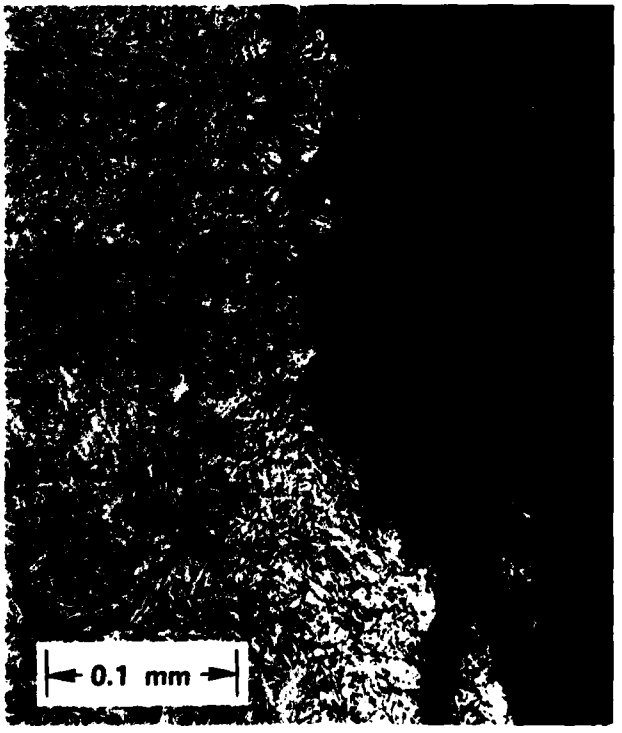

(b) HY-100 SAW (55 kJ/in.)

(c) HY-100 SAW (110 kJ/in.)

Figure 7 - Crack Surfaces of HY-100 Steel Plate and Weldment Specimens Tested in Natural Seawater Coupled to Zinc Anode

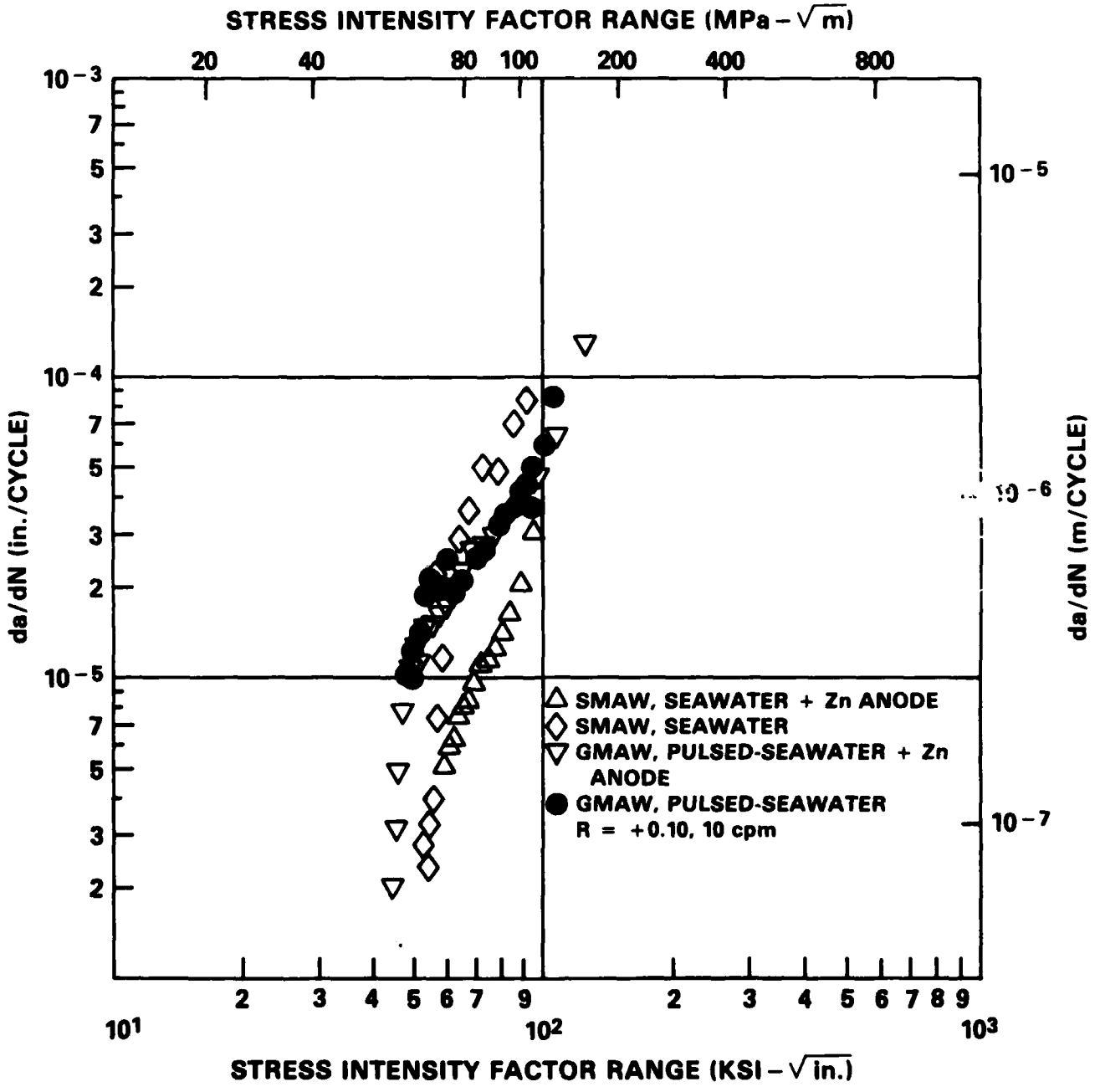

Figure 8 - Fatigue Crack-Growth Rates for HY-100 Steel SMAW and GMAW-Pulsed Arc Weld Metals with Heat Inputs Nominally 55 kJ/in. in Natural Seawater, Freely Corroding and Coupled to Zinc Anode

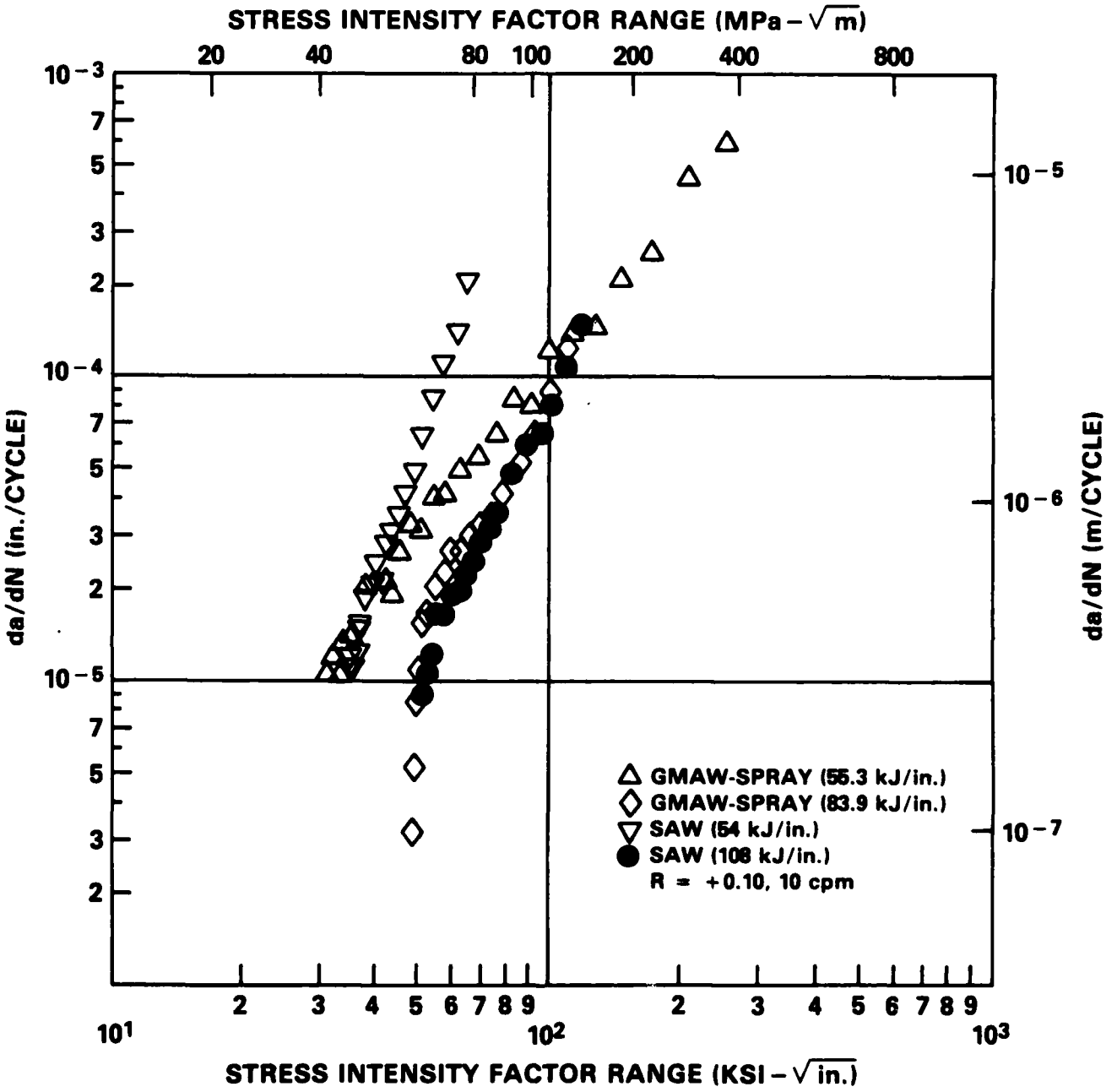

Figure 9 - Fatigue Crack-Growth Rates for HY-100 Steel GMAW-Spray and SAW Weld Metals Prepared with High and Normal Heat Inputs in Natural Seawater Coupled to Zinc Anode

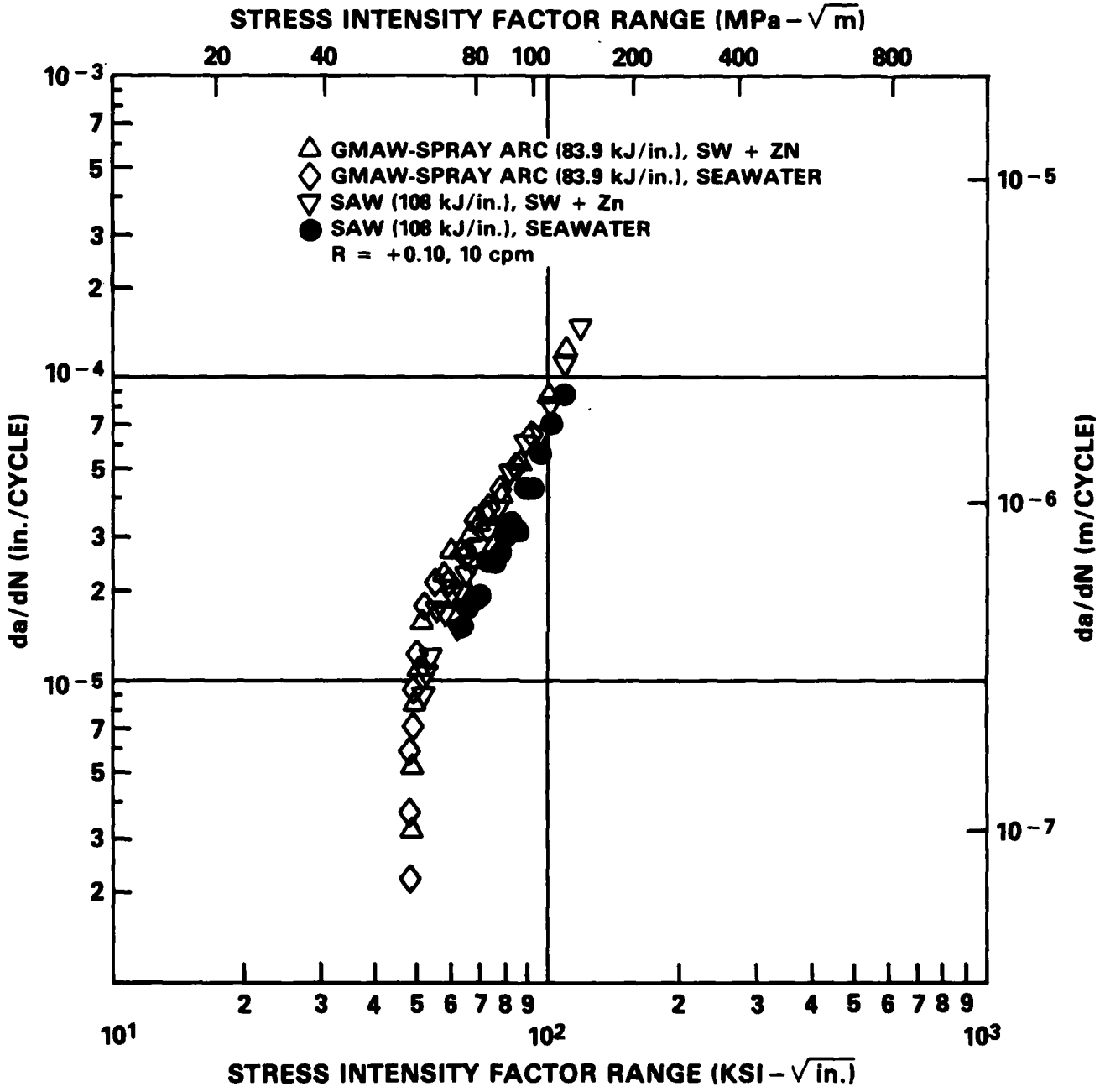

Figure 10 - Fatigue Crack-Growth Rates for HY-100 Steel GMAW-Spray Arc and SAW Weld Metals Prepared with High Heat Inputs in Natural Seawater, Freely Corroding and Coupled to Zinc Anodes

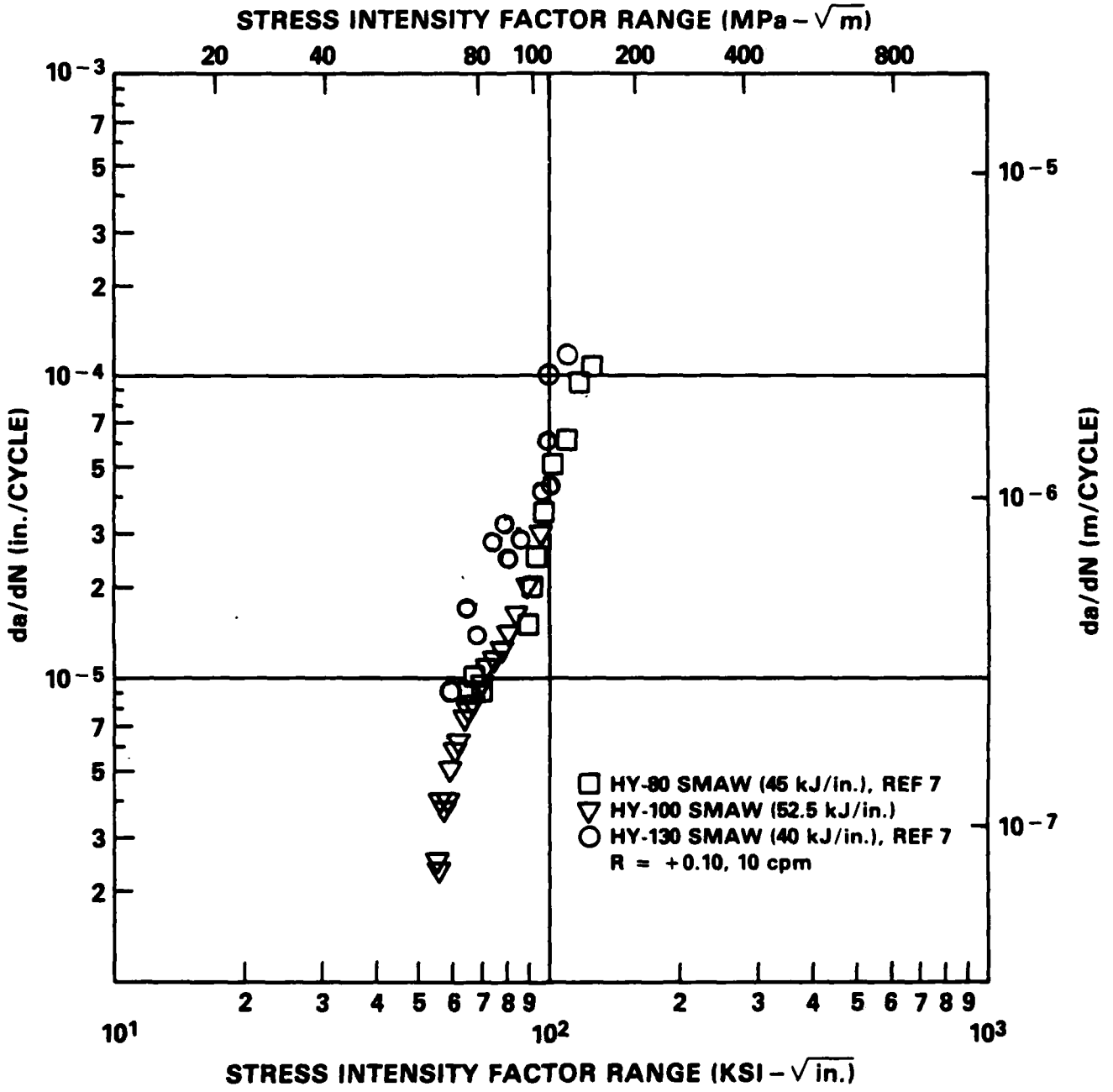

Figure 11 - Fatigue Crack-Growth Rates for HY-80, HY-100, and HY-130 Steel Weld Metals (Heat Input Nominally 45 to 50 kJ/in.) in Natural Seawater Coupled to Zinc Anode; HY-80 and HY-130 Data Taken From Reference 7.

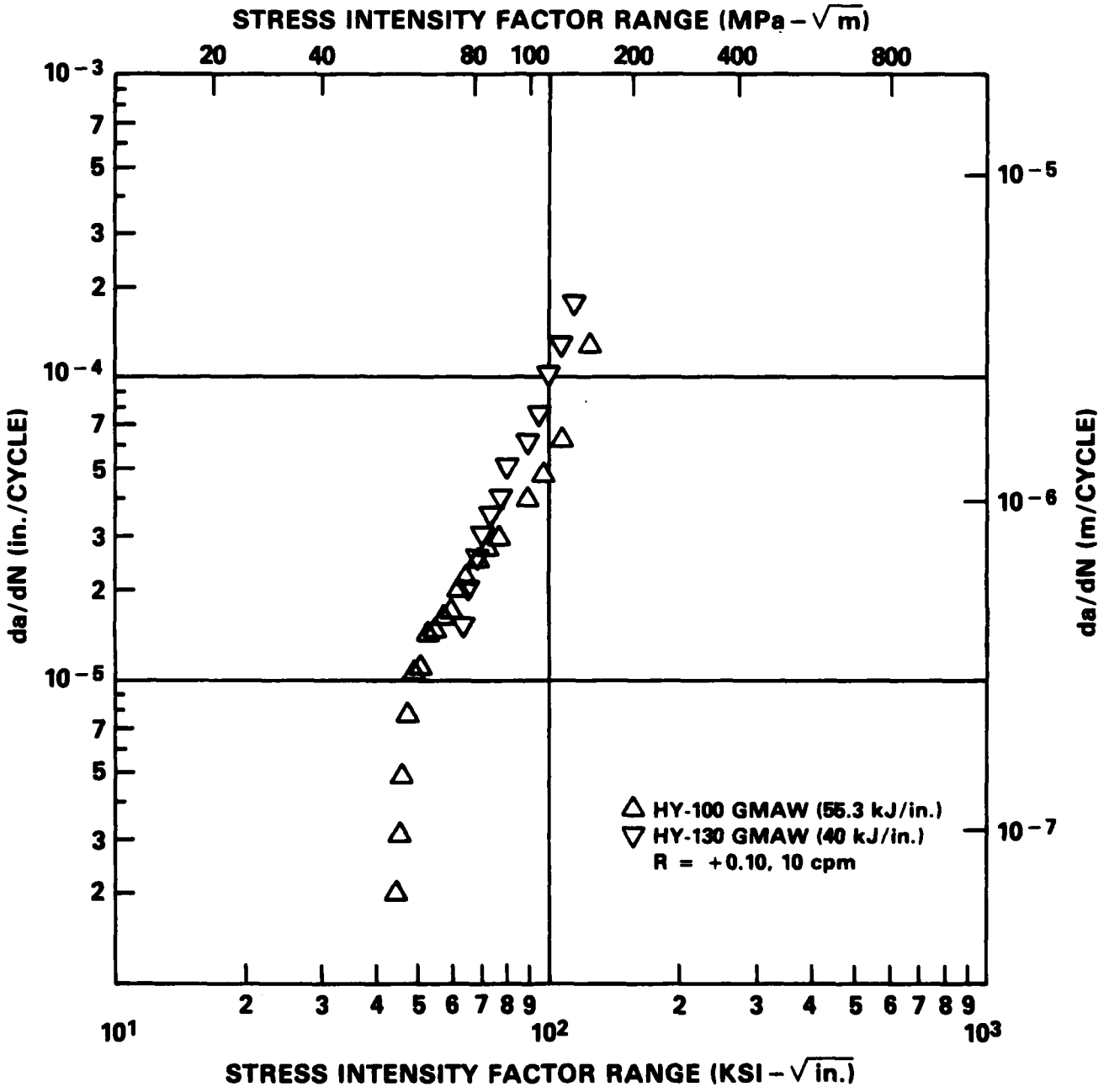

Figure 12 - Fatigue Crack-Growth Rates for HY-100 and HY-130 Steel GMAW Weld Metals (Heat Input Nominally 40 to 55 kJ/in.) in Natural Seawater Coupled to Zinc Anode, HY-130 Data Taken From Reference 7.

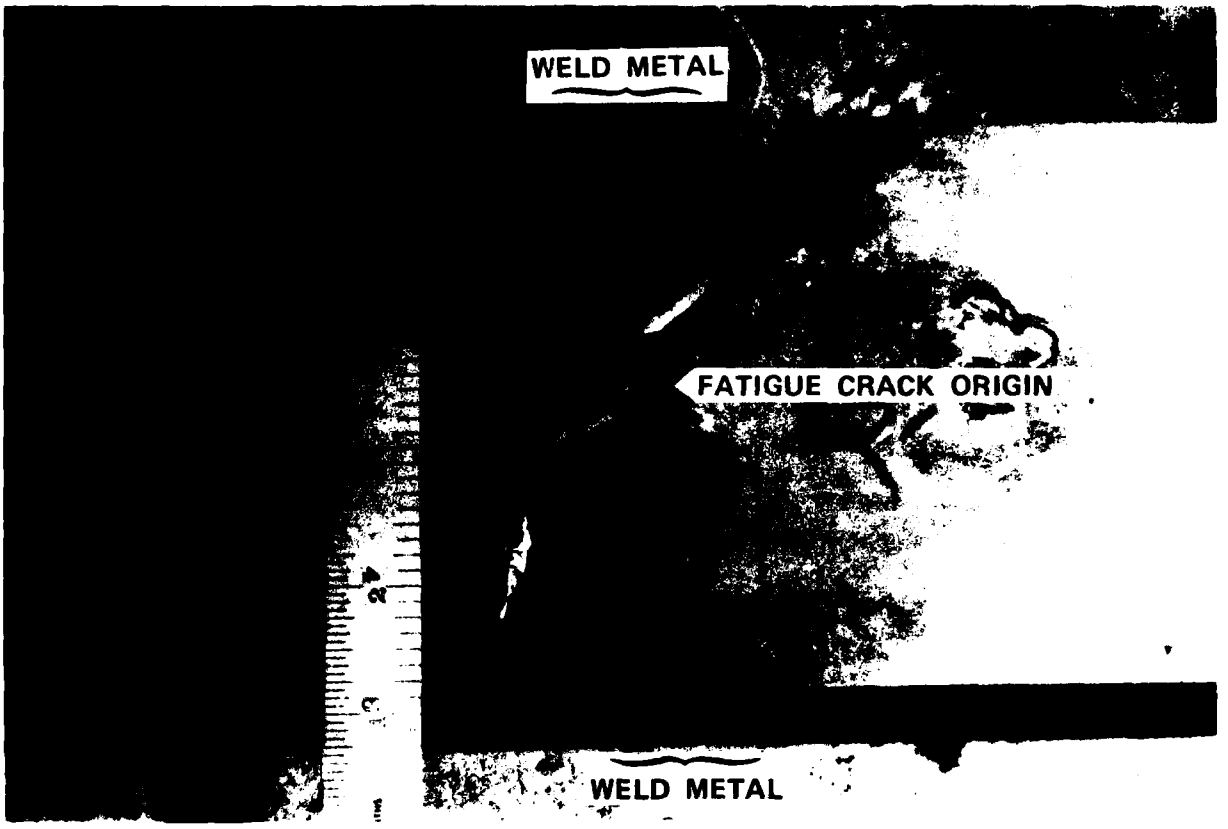

Figure 13 - Fatigue Failure of HY-100 Steel GMAW Welded Beam With Reinforcement Removed Prior to Fatigue Test

REFERENCES

1. Gross, M.R., "Low-Cycle Fatigue of Materials for Submarine Construction," Naval Engineers Journal (Oct 1963) pp. 783-797.

2. Gross, M.R. and E.J. Czyryca, "Effects of Notches and Saltwater Corrosion on the Flexural Fatigue Properties of Steels for Hydrospace Vehicles," Naval Engineers Journal (Dec 1967) pp. 1003-1013.

3. Radziminski, J.B. and F.V. Lawrence, Jr., "Fatigue of High Yield-Strength Weldments," Welding Research Supplement (Aug 1970) pp. 365s-375s.

4. Knight, J.W., "Corrosion Fatigue of Welded Quenched and Tempered Steels," Welding Research International, Vol. 7, No. 5 (1977) pp. 385-411.

5. Yoder, G.R., et al., "Procedures for Precision Measurement of Fatigue Crack Growth Rate Using Crack-Opening Displacement Techniques," Fatigue Crack Growth Measurement and Data Analysis, ASTM STP 738 (1981) pp. 85-102.

6. Saxena, A. and S.J. Hudak, Jr., "Review and Extension of Compliance Information for Common Crack Growth Specimens," International Journal of Fracture, Vol. 14, No. 5 (Oct 1978) pp. 453-468.

7. Davis, D.A. and Czyryca, E.J., "Corrosion Fatigue Crack-Growth Properties of HY-130 Steel and Weldments," Transactions of the ASME, Journal of Pressure Vessel Technology, Vol. 103, No. 4 (Nov 1981) pp. 314-321.

8. Crooker, T.W., et al., "Effects of Flowing Natural Seawater and Electrochemical Potential of Fatigue Crack Growth in Several High-Strength Marine Alloys," Corrosion-Fatigue Technology, STP 642, ASTM (1978) pp. 189-201.

9. Vosikovsky, O., "Frequency, Stress Ratio, and Potential Effects on Fatigue Crack Growth of HY-130 Steel in Saltwater," Journal of Testing and Evaluation, Vol. 6, No. 3 (May 1978) pp. 175-182.

10. Clarke, W.G. Jr. and D.S. Kim,, "Effect of Synthetic Seawater on the Crack Growth Properties of HY-130 Steel Weldments," Engineering Fracture Mechanics, Vol. 4 (1972) pp. 499-510.

11. Parry, M., et al., "Fatigue Crack Propagation in A514 Base Plate and Welded Joints," Welding Journal Research Supplement (Oct 1972) pp. 485s-490s.

INITIAL DISTRIBUTION

Copies	
4	NRL
	1 Code 6300
	1 Code 6380
	2 Code 6384
18	NAVSEA
	1 (SEA 05D)
	2 (SEA 05M)
	1 (SEA 05R)
	2 (SEA 05R25)
	2 (SEA 08)
	1 (SEA 32B)
	1 (SEA 323)
	2 (SEA 3232)
	2 (SEA 3233)
	1 (SEA 92)
	1 (PMS 393)
	2 (SEA 99612)
1	NISC (Code 369)
12	DTIC

CENTER DISTRIBUTION	
Copies	Code
1	17
1	172
1	1720.3
2	1720.4
1	173
1	1730.2
1	1730.6
1	28
2	2803
1	2809H
5	281
15	2814
1	282
2	2821
1	522.1
2	5231